Progress towards 14% Efficient CdTe Solar Cells in Substrate Configuration

Lukas Kranz[1], Rafael Schmitt[1], Christina Gretener[1], Julian Perrenoud[1], Fabian Pianezzi[1], Alexander R. Uhl[1], Debora Keller[1], Stephan Buecheler[1], Ayodhya N. Tiwari[1]

[1]Empa – Swiss Federal Laboratories for Materials Science and Technology, Laboratory for Thin Films and Photovoltaics, Ueberlandstrasse 129, Dübendorf, Switzerland

ABSTRACT — **CdTe solar cells are conventionally grown in superstrate configuration. However, the growth in substrate configuration offers more control of junction properties as recrystallization of CdTe and junction formation with CdS can be decoupled. In this paper the influence of various annealing treatment conditions of the CdS layer on its morphology and phase and on the device properties is presented. The presence of $CdCl_2$ during this annealing treatment is important for the phase change of the CdS layer to hexagonal wurtzite and for high efficiencies. A $CdCl_2$ treatment of the CdS at 360 °C improves the efficiency of the device without the adverse effect of pinhole formation in the CdS. CdTe solar cells in substrate configuration with more than 13% efficiency are achieved as a progress towards 14% efficiency.**

Index Terms **— II-VI semiconductor materials, Heat treatment, Solar energy, Thin film devices.**

I. Introduction

CdTe is one of the most attractive materials for production of low cost thin film solar modules. Conventionally, CdTe solar cells are grown in superstrate configuration. However, the growth in substrate configuration offers the possibility of choosing a variety of substrate materials including metal foils, which enable high-throughput roll-to-roll manufacturing. Furthermore, substrate configuration offers more control of junction properties as CdS is deposited after recrystallization of CdTe. This has several advantages for independent optimization of the electronic properties and the junction formation. In spite of these advantages, the growth in substrate configuration has so far resulted in significantly lower efficiencies than in superstrate configuration, typically well below 10% and a few examples crossing 10% efficiency [1,2].

An important processing step for the growth of CdTe solar cells is the junction formation. In superstrate configuration, the junction is formed during the $CdCl_2$ treatment of the CdS/CdTe layer stack, which also leads to the recrystallization of the CdTe and CdS layers. While this process is well established, the best junction formation process for substrate configuration is under debate. Various approaches were used for substrate configuration, e.g. a $CdCl_2$ treatment only after CdTe [1-3], a $CdCl_2$ treatment of the CdTe-CdS layer stack [4], or a $CdCl_2$ treatment after both CdTe and CdS [1,3,5].

We obtain best performance with separate $CdCl_2$ treatments of the CdTe and CdS. This approach enables independent control over the recrystallization of the CdTe and the junction formation with CdS. We show that the presence of $CdCl_2$ is important during the annealing treatment of the CdS and that the oxygen content of the annealing ambient has to be controlled. Furthermore, we show that the addition of a second CdS layer after the annealing treatment of the first CdS layer improves open circuit voltage (V_{OC}) and fill factor (FF). Performing the $CdCl_2$ treatment at 360 °C improves the electronic properties without adverse effect on the microstructure of CdS. Substrate configuration CdTe solar cells with efficiency of more than 13% are produced.

II. Experimental

CdS/CdTe solar cells in substrate configuration were grown on Mo/MoO_x covered Corning 7059 glass. In some cases a Te layer was added on top of the MoO_x. CdTe was deposited by vacuum evaporation at 350 °C followed by a recrystallization and doping treatment [6]. CdS was deposited by chemical bath deposition (CBD). A $CdCl_2$ treatment of the CdS was performed by vacuum evaporation of 100 nm of $CdCl_2$ followed by annealing at different temperatures and oxygen contents of the annealing ambient as stated in the text. In some cases a second CdS layer was deposited by chemical bath deposition. A double layer of i-ZnO/ZnO:Al was deposited by sputtering followed by a Ni/Al grid and MgF_2 anti-reflection coating by electron beam evaporation.

The performance of the solar cells was measured with current density voltage (J-V) measurements under simulated standard test conditions in a sun simulator and quantum efficiency (QE) measurements were performed for spectral mismatch correction.

Scanning electron microscopy (SEM) images of the first CdS layer deposited on glass/Mo/MoO_x/CdTe and annealed under different conditions were acquired with a Hitachi S-4800 operated at an accelerating voltage of 5 kV.

Samples for scanning transmission electron microscopy (STEM) were prepared by mechanical polishing of cross-sections followed by Ar ion milling using a Fischione TEM ion mill 1050 employing the liquid nitrogen cooling option. STEM analysis was performed on a JEOL 2200FS TEM/STEM operated at 200 kV.

TABLE I

PHOTOVOLTAIC (PV) PARAMETERS OF CDTE SOLAR CELLS PROCESSED WITH DIFFERENT CDS ANNEALING CONDITIONS.

Annealing conditions of 1st CdS layer			**2nd CdS layer**	**PV parameters**				**SEM image**
Temp. °C	O_2 vol %	$CdCl_2$		V_{OC} mV	J_{SC} mA/cm^2	FF %	Eff. %	
No annealing			no	703	20.1	54.4	7.7	a
400	50	yes	**no**	812	21.6	67.1	11.8	b
400	50	yes	**yes**	830	20.2	72.5	12.2	-
400	**30**	yes	yes	688	21.3	64.6	9.5	c
400	**80**	yes	yes	709	21.4	65.8	9.9	d
400	50	**no**	yes	711	20.5	59.8	8.7	e

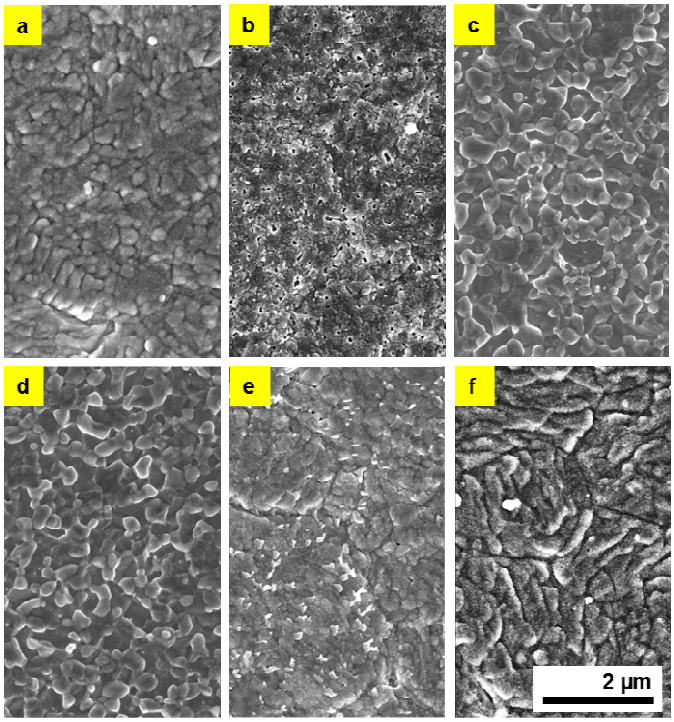

Fig. 1. Top view SEM images of as-deposited CdS on CdTe (a) and CdS deposited on CdTe and annealed under different conditions (b-f). All SEM figures show the morphology of the 1st CdS layer without addition of a 2nd CdS. Annealing conditions of b-e are shown in Table I. Sample f is processed at 360 °C, 50% O_2, with $CdCl_2$.

In-situ X-ray diffraction (XRD) patterns were recorded using a PANanalytical XPert Pro MPD X-ray diffractometer. A 2θ scan was recorded with fixed grazing incidence angle of 3°. XRD patterns of a solar cell processed up to the first CdS layer were recorded at temperatures between 150 °C and 450 °C (10 °C steps, 1.5°C/min ramping speed) in an ambient containing 50% of oxygen. The experiment was performed both with and without a $CdCl_2$ layer on the CdS.

III. RESULTS AND DISCUSSION

Fig. 1 shows the top view SEM micrographs of CdS layers, which were deposited on the CdTe layer of solar cells in substrate configuration and annealed under different conditions. Table I shows the photovoltaic parameters of the corresponding finished devices. As-deposited CdS grown by CBD covers the CdTe layer with nanocrystalline sized grains (Fig. 1a). Upon a $CdCl_2$ treatment at 400 °C and 50% of O_2, the microstructure of the CdS layer significantly changes (Fig. 1b): Grain size increases and pinholes are formed in the CdS layer. In spite of the pinhole formation in the CdS layer, the efficiency of the solar cells increases due to improvements in all photovoltaic parameters, especially V_{OC} and FF.

Even though the $CdCl_2$ treatment of the CdS increases efficiency, the pinholes in the CdS layer which occur upon $CdCl_2$ treatment are detrimental to device performance due to the direct contact between CdTe and ZnO. In order to cover the pinholes and to enable a covering CdS layer, a second CdS layer is grown after the $CdCl_2$ treatment of the first CdS layer. Even though this leads to increased parasitic absorption in the CdS window layer and therefore a reduced short circuit current density (J_{SC}), with the application of the second CdS layer V_{OC} and FF are further increased. V_{OC} well above 800 mV and FF above 70% are obtained (Table I), leading to an increased efficiency of 12.2%.

We have varied the oxygen content during the $CdCl_2$ treatment of the CdS and have investigated its influence on the CdS morphology and the device performance. The oxygen content has a strong influence on the CdS morphology and changing the oxygen content from 50% to 30% or 80% leads to pronounced pinhole formation (Fig. 1c & d). The efficiency is reduced to below 10% due to a reduction of V_{OC} and FF. This shows, that oxygen content during the annealing treatment at 400 °C has to be well controlled in order to achieve a good morphology of the CdS with minimal pinhole density and to obtain high efficiencies.

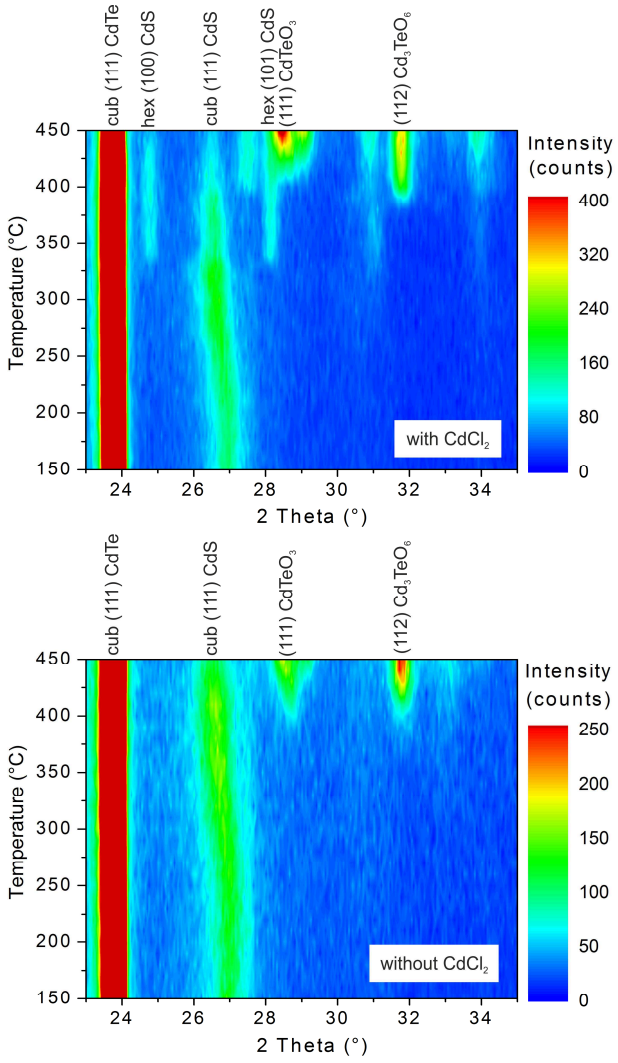

Fig. 2. In-situ XRD patterns during the $CdCl_2$ treatment of CdS (a) and while annealing without the presence of $CdCl_2$ (b). CdS was deposited on a Glass/Mo/MoO_x/CdTe layer stack.

Grain growth is a typical influence of the $CdCl_2$ treatment and can lead to pinhole formation. In an attempt to avoid pinhole formation, a sample was identically processed as the device with 12.2% efficiency but without addition of $CdCl_2$ during the annealing of the CdS. SEM images confirm that this significantly reduces pinhole formation in the CdS (Fig. 1e). In spite of the improved coverage, a low V_{OC} of ~700 mV and a low FF of ~60% are obtained, yielding an efficiency of only 8.7% (Table I).

It is possible that the annealing conditions of the CdS (temperature, oxygen content) need to be adapted for an annealing step without $CdCl_2$. Therefore, we have produced several samples with varying annealing conditions of the CdS without addition of $CdCl_2$. The highest obtained efficiency for a solar cell where the CdS was annealed without addition of $CdCl_2$ is 11.1% (799 mV, 61.2% FF, 22.8 mA/cm^2). This is obtained by reducing oxygen content to 10% while the temperature is kept at 400 °C. The lower oxygen content reduces oxidation of the CdS, while a reduced oxygen content is not needed when $CdCl_2$ is used, which protects the CdS layer from oxidation [7]. The efficiencies of cells processed without addition of $CdCl_2$ during the annealing treatment of the CdS always remained significantly lower than what we achieve with addition of $CdCl_2$, especially due to a low FF<65% in samples without addition of $CdCl_2$. Therefore, we conclude, that addition of $CdCl_2$ during the annealing treatment of the CdS is important for good device performance, especially to obtain high FF.

Even when no $CdCl_2$ is added to the aforementioned samples, a small amount of $CdCl_2$ due to residuals in the annealing oven cannot be excluded. A sample similarly processed as the aforementioned sample with 11.1% efficiency shows significantly lower efficiencies when the CdS annealing treatment is performed after removing all residual $CdCl_2$ from the annealing oven. This further emphasizes the importance of the presence of $CdCl_2$ during the annealing treatment of the CdS.

To investigate the influence of the presence of $CdCl_2$ on the crystallographic phase of CdS we have performed in-situ XRD measurements of a solar cell processed up to the CdS with and without using $CdCl_2$ (Fig. 2). In the presence of $CdCl_2$ the phase of the CdS layer changes from cubic to hexagonal while the phase change does not occur when no $CdCl_2$ is present even when higher than usual annealing temperatures are used. The results suggest that recrystallization of the CdS layer to hexagonal phase is important to obtain high efficiency solar cells. In-situ XRD shows that above 400 °C various oxides are formed. The shift of the CdS (111) phase towards smaller angles upon annealing is attributed to oxygen loss from the hydro-oxygenated CBD grown CdS. The reduction of oxygen content in the CdS layer upon $CdCl_2$ treatment is confirmed with secondary ion mass spectroscopy measurements (not shown).

The in-situ XRD results furthermore show, that the phase change of the CdS, which accompanies the improved device performance already occurs at around 330 °C, which is significantly lower than typical $CdCl_2$ treatment temperatures of 400-420 °C commonly applied for CdTe solar cells in superstrate configuration.

We have produced solar cells where the CdS layer was $CdCl_2$ treated at 360 °C. XRD measurements confirm that this temperature also enables the change of phase from cubic to hexagonal CdS. Furthermore as shown in Fig. 1f, the lower temperatures enable an improved coverage of the CdTe layer with hexagonal CdS compared to the application of 400 °C. Top view SEM images do not reveal a significant change in morphology of the CdS layer upon $CdCl_2$ treatment of the CdS at 360 °C. However, TEM shows grain growth of the CdS upon $CdCl_2$ treatment at 360 °C (Fig. 3). The STEM image shows the double CdS layer between the CdTe absorber and the ZnO front contact. The first, $CdCl_2$ treated CdS layer exhibits grain size up to several 100 nm while the additional

CdS layer exhibits nanocrystallites as commonly observed for CBD grown CdS.

Fig. 4 shows the J-V and QE curve of a cell where the $CdCl_2$ treatment of the CdS is performed at 360 °C. An efficiency of 13.2% is obtained with V_{OC} and FF as high as the internal record efficiency cell in superstrate configuration [8], which is shown for comparison. It is also notable, that the rollover, which is generally very pronounced for CdTe solar cells in substrate configuration, is not observed for the cell with CdS bi-layer.

Even though the modified annealing treatment solves the structural problems of pinhole formation in the CdS, the second CdS layer is still required for highest V_{OC} and FF. Fig. 4 shows the J-V and QE curves of a cell without second CdS which has 13.3% efficiency. Remarkable V_{OC} and FF are reached, however the values are still lower compared to cells with CdS bi-layer.

The presence of $CdCl_2$ during the annealing treatment of the CdS is crucial for highest performance and in-situ XRD reveals that the presence of $CdCl_2$ is needed to obtain a phase change of CdS upon annealing. Furthermore, all high efficiency devices, which were investigated by XRD, had hexagonal CdS. This could hint towards the important role of the hexagonal phase of CdS. However, XRD measurements of a high efficiency superstrate cell revealed cubic CdS. These results indicate that another effect accompanies the phase change of CdS, possibly the diffusion of elements or the modification of the CdS/CdTe interface, which lead to improved electronic properties. This will be discussed in future publications.

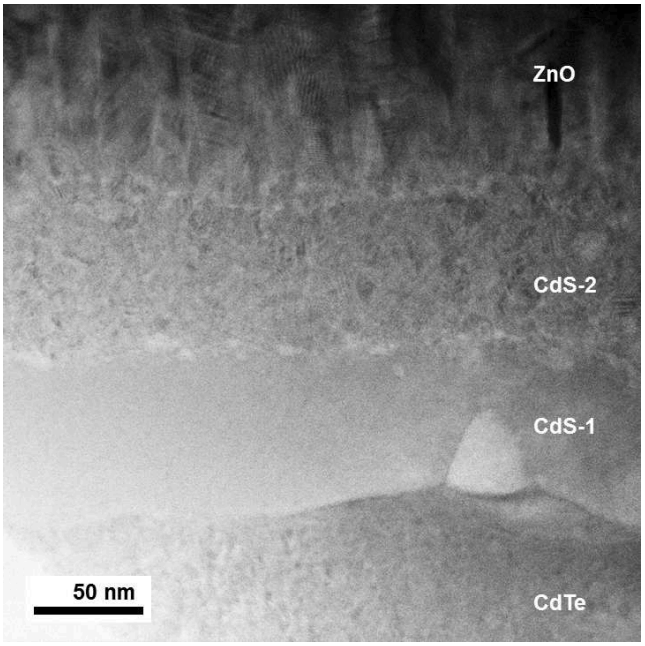

Fig. 3. Bright field STEM image of the double layer CdS in a CdTe solar cell. The first CdS layer (CdS-1) is $CdCl_2$ treated at 360 °C and the second CdS (CdS-2) is as-deposited CBD grown CdS.

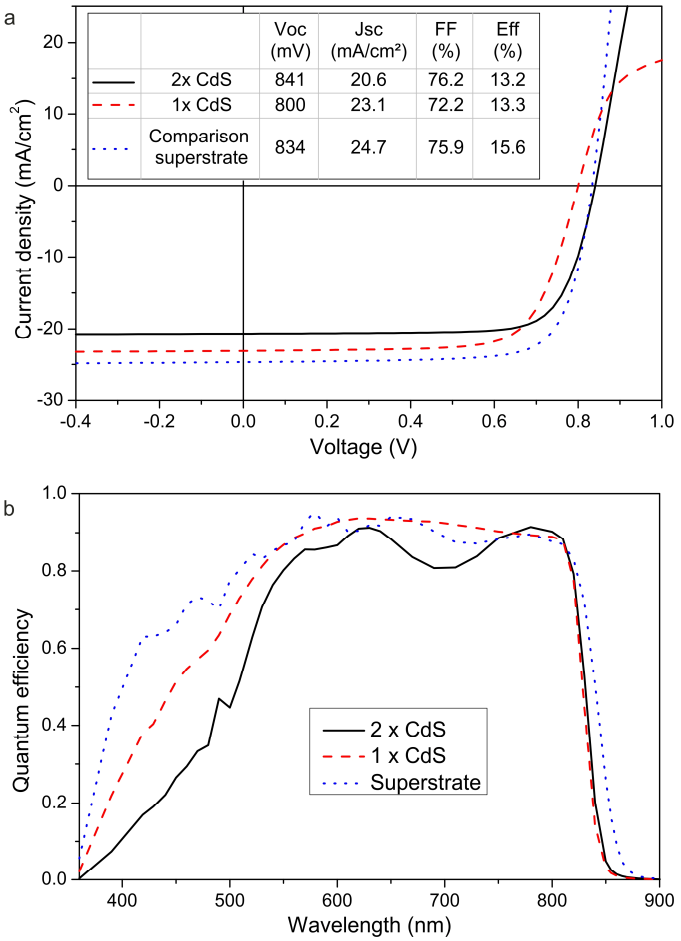

Fig. 4. J-V (a) and QE (b) measurements of cells processed with a $CdCl_2$ treatment of the CdS at 360 °C with single and double CdS layer. Our internal record cell in superstrate configuration is included for comparison [8]. The inset shows the PV parameters of the corresponding cells

The results of high V_{OC} and FF of the cell with CdS bi-layer and the high J_{SC} of the cell with single CdS (Fig. 4) suggest that efficiencies well above 14% should be achievable. However, the increase in J_{SC} upon CdS thickness reduction was accompanied by a decrease in V_{OC} and FF so far. In future we will test different approaches to achieve a reduction of CdS thickness without loss in V_{OC} and FF.

III. Summary & Outlook

In conclusion, the influence of different processing conditions during an annealing treatment after deposition of the CdS layer on its morphology and phase as well as on the device properties is investigated. The presence of $CdCl_2$ during the annealing treatment of the CdS is important for a phase change of the CdS to hexagonal phase and for high efficiency solar cells. Oxygen content during this annealing treatment has to be well controlled to achieve good CdS morphology and for improved device performance.

Performing the $CdCl_2$ treatment at 360 °C leads to a phase change of the CdS without adverse effects on the coverage of CdS. CdTe solar cells in substrate configuration with more than 13% efficiency are achieved. In future publications the effect of the annealing treatment on electronic properties and diffusion of impurities will be further elaborated. Furthermore, we will test different approaches to reduce CdS layer thickness or to substitute CdS by alternative materials in order to further increase efficiency towards and beyond 14%.

REFERENCES

[1] C. Gretener, J. Perrenoud, L. Kranz, L. Kneer, R. Schmitt, S. Buecheler, and A. N. Tiwari, "CdTe/CdS thin film solar cells grown in substrate configuration," *Prog. Photovolt.,* DOI: 10.1002/pip.2233, 2012.

[2] J. N. Duenow, R. G. Dhere, D. Kuciauskas, J. V. Li, J. W. Pankow, P. C. Dippo, C. M. DeHart, and T. A. Gessert, "Oxygen incorporation during fabrication of substrate CdTe photovoltaic devices," *38th IEEE Photovoltaic Specialists Conference,* pp. 3225-3229, 2012.

[3] R. G. Dhere, J. N. Duenow, C. M. DeHart, J. V. Li, D. Kuciauskas, M. R. Young, K. Alberi, A. Mascarenhas and T. A. Gessert, "Analysis of the junction properties of CdS/CdTe devices in substrate and superstrate configurations," *Proc. 26th Europ. Photovolt. Solar Energy Conf.,* pp. 2456-2459, 2011.

[4] I. Matulionis, S. Han, J. A. Drayton, K. J. Price and A. D Compaan, "Cadmium Telluride Solar Cells on Molybdenum Substrates," *Proc. Mater. Res. Soc. Symp.* 668, H8.23, 2001.

[5] V. P. Singh, J. C. McClure, G. B. Lush, W. Wang, X. Wang, G. W. Thompson and E. Clark, "Thin film CdTe-CdS heterojunction solar cells on lightweight metal substrates," *Solar Energy Materials & Solar Cells* 59, pp. 145-161, 1999.

[6] L. Kranz et al., submitted

[7] L. Wan, Z. Bai, Z. Hou, D. Wang, H. Sun, and L. Xiong, "Effect of $CdCl_2$ annealing treatment on thin CdS films prepared by chemical bath deposition," Thin Solid Films, 518, 23, pp. 6858-6865, 2010.

[8] J. Perrenoud, L. Kranz, S. Buecheler, F. Pianezzi and A. N. Tiwari, "The use of aluminum doped ZnO as transparent conductive oxide for CdS/CdTe solar cells," Thin Solid Films 519, pp. 7444-7448, 2011.